



International Symposium on
Ultrasonic Imaging and
Tissue Characterization



Dual-robotic Arm Prostate Ultrasound Tomography

Students:

Yunpu Zhang, Zhenghao Li, Ziyi Wang

Mentors:

Yixuan Wu, Mohammad Salehizadeh,
Dr. Russ Taylor, Dr. Emad Boctor



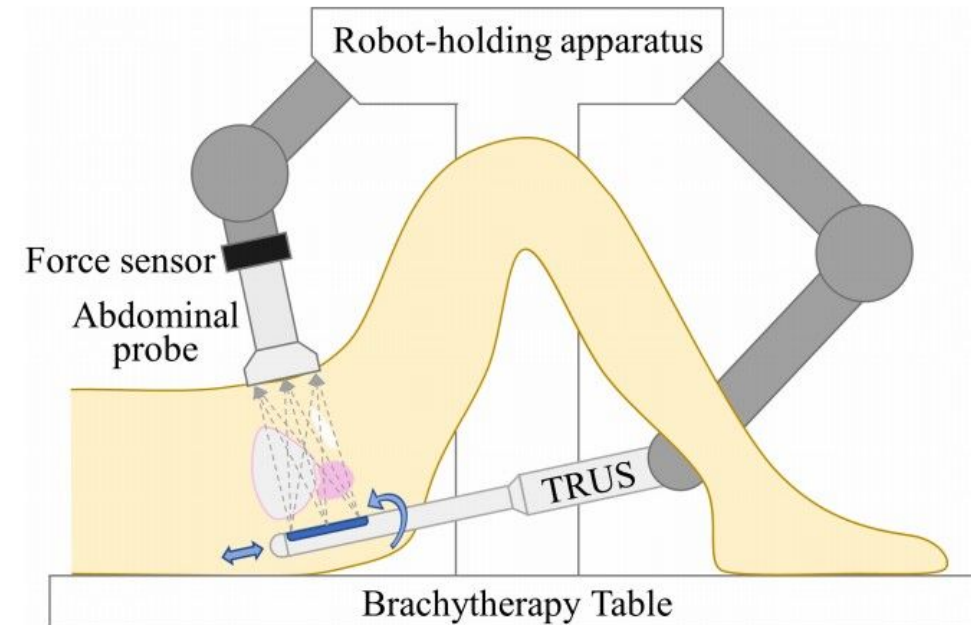
JOHNS HOPKINS
UNIVERSITY



JOHNS HOPKINS
SCHOOL of MEDICINE

Title: Dual-robotic Arm Prostate Ultrasound Tomography

Goal: A dual robotic system with an aligned abdominal and a TRUS probe used for prostate cancer detection.



Gilboy, Kevin Michael. ROBOTIC ULTRASOUND TOMOGRAPHY AND COLLABORATIVE CONTROL. 2020, https://drive.google.com/file/d/19cGn_ZnCLbUESI9dta3l0s91Qdg-DwQI/view?usp=sharing.

Second Paper -> Choose phantoms and Calibration method

Zhang, Haichong K., et al. 'Phantom with Multiple Active Points for Ultrasound Calibration'. J. Med. Imag. 5(4), 045001 (2018), Doi: 10.1117/1.JMI.5.4.045001., 2022b, <https://pubmed.ncbi.nlm.nih.gov/30525061/>.

First Paper -> Motion Planning and Calibration

Gilboy, Kevin M., et al. Dual-Robotic Ultrasound System for In Vivo Prostate Tomography. 2020, https://link.springer.com/chapter/10.1007/978-3-030-60334-2_16.

Third Paper -> Moving the robot **safely** to desired position with certain orientation

Ming Li, A. Kapoor and R. H. Taylor, "A constrained optimization approach to virtual fixtures," *2005 IEEE/RSJ International Conference on Intelligent Robots and Systems*, Edmonton, AB, Canada, 2005, pp. 1408-1413, doi: 10.1109/IROS.2005.1545420.

PAPER#1: DUAL-ROBOTICS ULTRASOUND SYSTEM FOR IN VIVO PROSTATE TOMOGRAPHY

Background:

Prostate cancer is the fifth leading cause of cancer death for males, and early detection is crucial for effective treatment.

Challenges:

PSA blood test: Not accurate
multi-parametric MRI: Expensive



Water tanks:
Hard to obtain high-resolution image

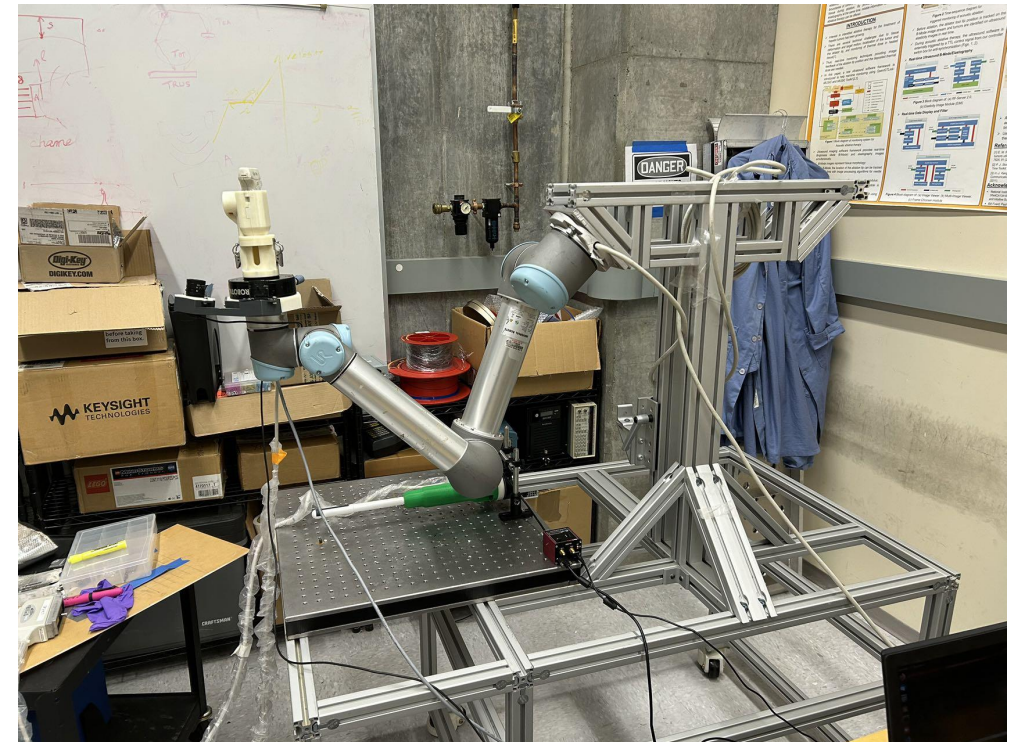
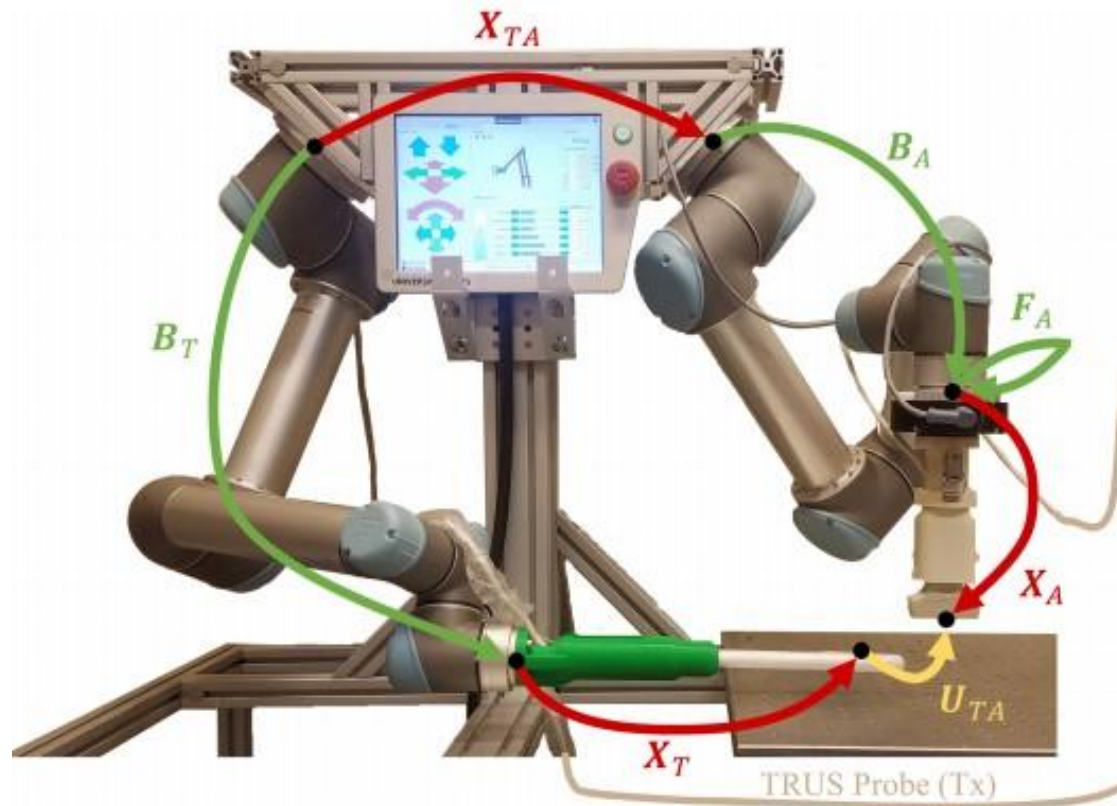


Solutions:

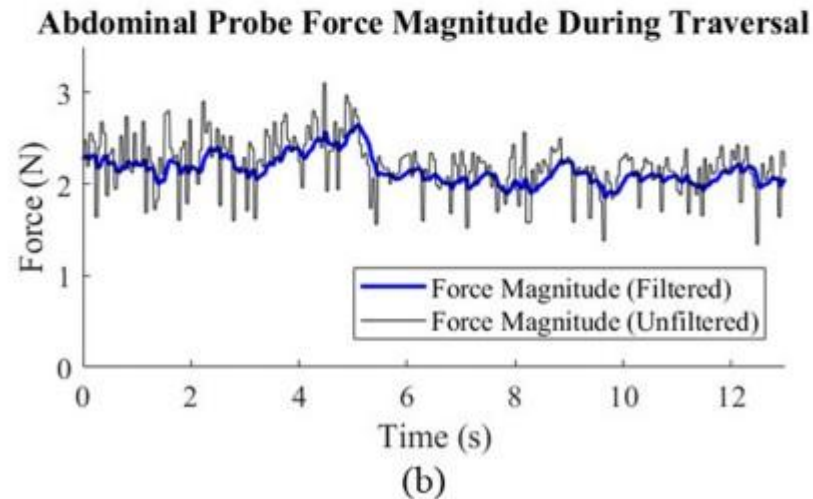
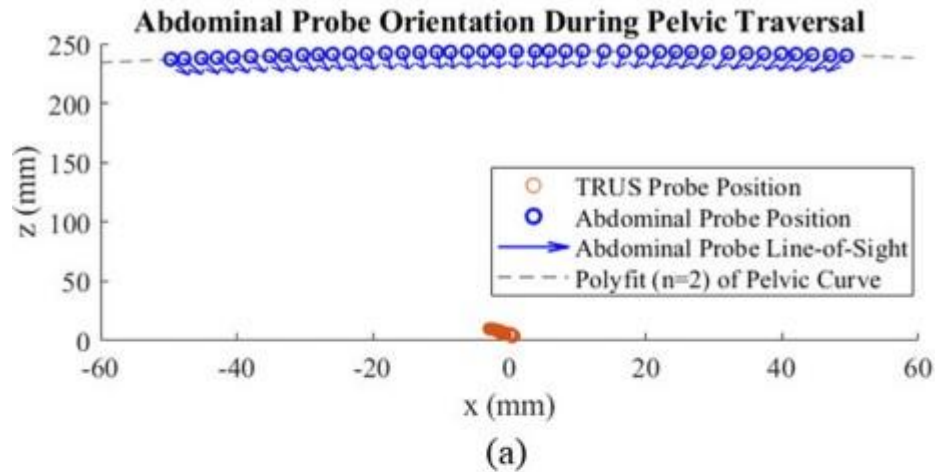
Ultrasound computed tomography
(USCT) technology:
real-time, non-invasiveness, and high
image resolution

Dual-robotic arm system:
suitable for prostate cancer
detection

Calibration method and revise:



Gilboy, Kevin M., et al. Dual-Robotic Ultrasound System for In Vivo Prostate Tomography. 2020, https://link.springer.com/chapter/10.1007/978-3-030-60334-2_16.



Calibration:

- The error of the transformation X_A and X_T is $0.13 \text{ mm} \pm 0.08 \text{ mm}$ and $0.52 \text{ mm} \pm 0.30 \text{ mm}$ respectively.
- X_{TA} resulting in $0.58 \text{ mm} \pm 0.32 \text{ mm}$ error.

Motion framework:

- The abdominal probe was able to track the motion of the TRUS probe.
- The abdominal probe maintained continuous contact with phantom with constant, gentle forces.

Robot Motion Framework:

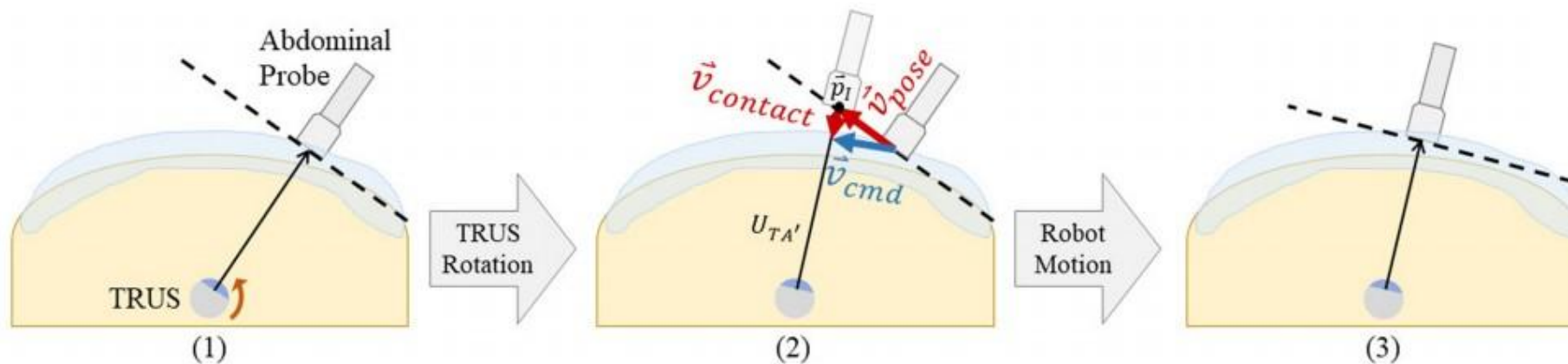
$$\mathbf{v}_{cmd} = \mathbf{v}_{pose} + \mathbf{v}_{contact}$$

$\mathbf{V}_{contact}$:

- Obtain from impedance control
- $\mathbf{v}_{contact} = K(F_D - F) - D(\dot{F})$

\mathbf{V}_{pose} :

- Derivative of the estimated pose with respect to time



Pros:

- Successful implementation to achieve the precise alignment between two probes, allowing for relatively accurate imaging results.
- Fully automatic, without hand guide to adjust the force applied to the phantom.

Cons:

- Not quantify the accuracy required by USCT.
- Using png image for BXp calibration.

Takeaways:

- Calibration part need to be revised due to our dependencies.
- Motion framework part is used to find P_{goal} , and velocity calculation is replaced by virtue fixture methods.

INTRODUCTION AND BACKGROUND

Traditional phantoms for ultrasound calibration:

1. Point-based phantoms. (More accurate, requires mid-plane search process. No rotational information, Bxp)
2. Structure-based Phantoms such as a line(s) or wall(s). (Full pose, but enlarge the error due to inaccurate feature segmentation)

What traditional calibration methods may not be sufficient:

1. Complex structures.
2. Multiple locations within the body.

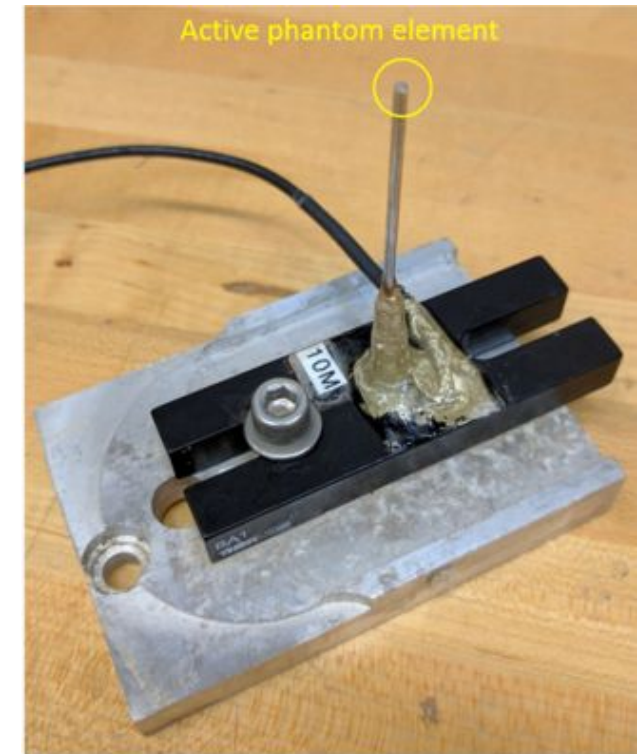
Need a more comprehensive calibration method.

Phantom with multiple active points for ultrasound calibration

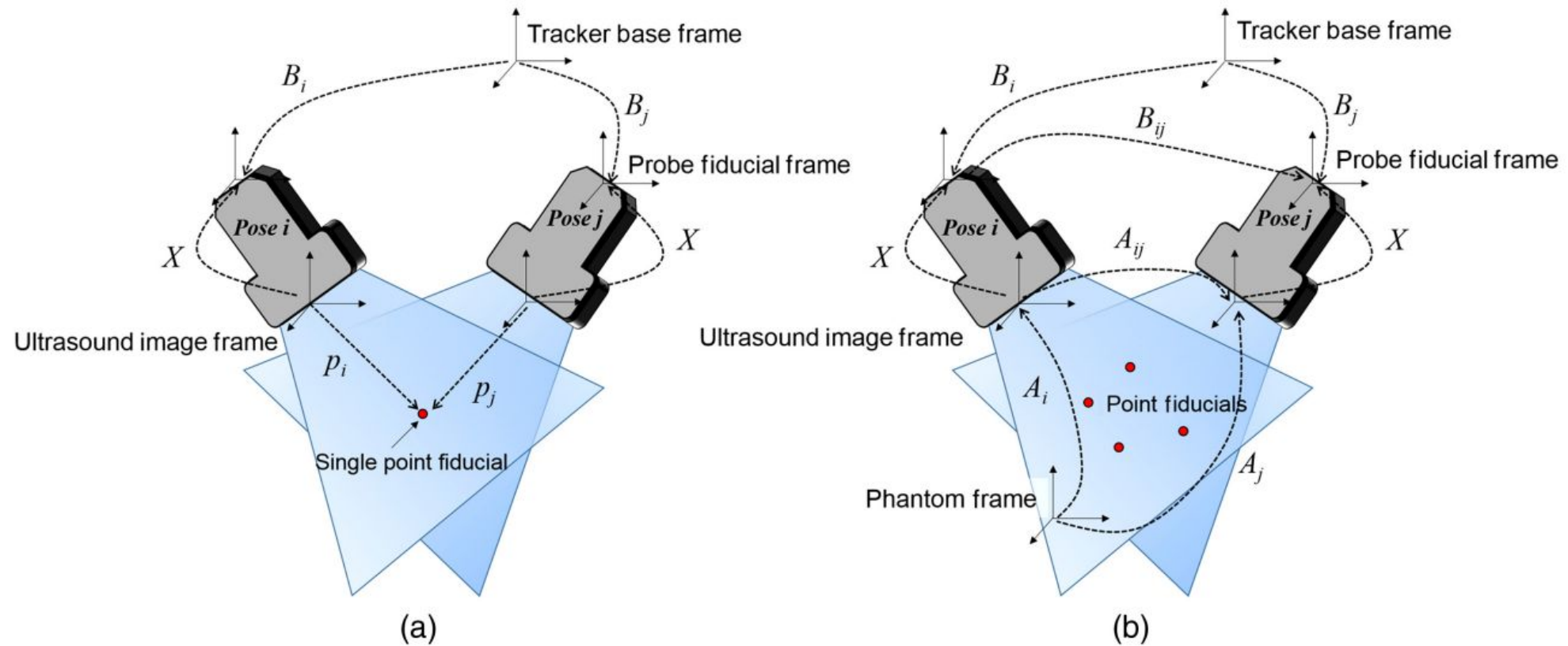
An active-point target: A point fiducial that can actively interact with the US receiver by transmitting acoustic waves.

Single piezoelectric (PZT) element. The PZT element transmits acoustic signals with a large capture range and can be received by the US probe even if the target is positioned out of plane.

Multiple active points = Coordinate frame, Full information and enabling the $AX = XB$ formulation.



Phantom with multiple active points for ultrasound calibration



Picture from [5]Zhang, Haichong K., et al. 'Phantom with Multiple Active Points for Ultrasound Calibration'. J. Med. Imag. 5(4), 045001 (2018), Doi: 10. 1117/1. JMI. 5. 4. 045001., 2022b, <https://pubmed.ncbi.nlm.nih.gov/30525061/>.

Phantom with multiple active points for ultrasound calibration

Table 1 The experimental results.

Calibration		Internal precision c (mm)	External precision c (mm)
Dual array (biplane)	<i>BXp</i> Point #1	0.77	2.55
	<i>BXp</i> Point #2	0.68	1.56
	<i>BXp</i> Point #3	0.79	3.59
	<i>BXp</i> Point #4	0.66	2.60
	<i>AXXB</i>	0.60	0.67
Mono (1-D) array	<i>AXXB</i>	0.93	0.98
Control (<i>BXp</i>) ¹⁴	<i>CW/AE</i>	1.72	—
	<i>AE/CW</i>	1.00	—

5 points

Internal precision c : The reconstruction precision computed on the 4 points used for calibration.

The external precision c : The reconstruction precision when the fifth independent point is used for evaluation.

New phantom using $AX=XB$, gives good internal and external precision. (And saved time)

Good internal precision by *BXp*.

X well optimized in area near the points, not far away!

Introduced different calibration methods with pros and cons for our project.

Provided simulation and experimental results for different phantoms and method.

Bxp algorithm with point fiducials is used.

1. Probe will be in the area near the calibration points when scanning the phantom.

2. New phantom requires a special hardware setup.

Phantom with multiple active elements with known geometric relationships.

One active element transmission system with translational motion needed.

(2-D translational stage)

New phantom will save time on midplane search, hard to build. (compared with crossed fishing wires)

Bxp is accurate enough. It is easier (phantom) and faster for our problem.

A Constrained Optimization Approach to Virtual Fixtures

Author: Ming Li, Ankur Kapoor, and Russell H. Taylor

Journal: *2005 IEEE/RSJ International Conference on Intelligent Robots and Systems*, Edmonton, AB, Canada, 2005, pp. 1408-1413, doi: 10.1109/IROS.2005.1545420.

Li, M., Taylor, R.H. (2003). Optimum Robot Control for 3D Virtual Fixture in Constrained ENT Surgery. In: Ellis, R.E., Peters, T.M. (eds) Medical Image Computing and Computer-Assisted Intervention - MICCAI 2003. MICCAI 2003. Lecture Notes in Computer Science, vol 2878. Springer, Berlin, Heidelberg. https://doi.org/10.1007/978-3-540-39899-8_21

Ming Li, A. Kapoor and R. H. Taylor, "A constrained optimization approach to virtual fixtures," *2005 IEEE/RSJ International Conference on Intelligent Robots and Systems*, Edmonton, AB, Canada, 2005, pp. 1408-1413, doi: 10.1109/IROS.2005.1545420.

Background:

The workspace in ENT (Ear, Nose, Throat) Surgery is very limited.

Challenges:

Sophisticated Geometric Constraints
Hard to Achieve Desired Position



Solutions:

A constrained quadratic optimization
algorithm

Li, M., Taylor, R.H. (2003). Optimum Robot Control for 3D Virtual Fixture in Constrained ENT Surgery. In: Ellis, R.E., Peters, T.M. (eds) Medical Image Computing and Computer-Assisted Intervention - MICCAI 2003. MICCAI 2003. Lecture Notes in Computer Science, vol 2878. Springer, Berlin, Heidelberg. https://doi.org/10.1007/978-3-540-39899-8_21

Ming Li, A. Kapoor and R. H. Taylor, "A constrained optimization approach to virtual fixtures," *2005 IEEE/RSJ International Conference on Intelligent Robots and Systems*, Edmonton, AB, Canada, 2005, pp. 1408-1413, doi: 10.1109/IROS.2005.1545420.

Optimization Algorithm

$$\begin{aligned} \arg \min_{\Delta \vec{q}/\Delta t} & \|W(\Delta \vec{x}/\Delta t - \Delta \vec{x}_d/\Delta t)\|, \\ \text{s.t. } & H\Delta \vec{x}/\Delta t \geq \vec{h}, \\ & \Delta \vec{x}/\Delta t = J\Delta \vec{q}/\Delta t \end{aligned} \quad (1)$$

Variable	Definition
W	Weight Matrix
H, h	Constraint Matrix
J	Manipulator Jacobian
$\Delta x, \Delta x_d$	Actual and Desired Change of a 6 by 1 Position Vector in Cartesian Space
Δq	Change of the 6 Joints Value on a UR5 (6 × 1 Vector) in Configuration Space

Li, M., Taylor, R.H. (2003). Optimum Robot Control for 3D Virtual Fixture in Constrained ENT Surgery. In: Ellis, R.E., Peters, T.M. (eds) Medical Image Computing and Computer-Assisted Intervention - MICCAI 2003. MICCAI 2003. Lecture Notes in Computer Science, vol 2878. Springer, Berlin, Heidelberg. https://doi.org/10.1007/978-3-540-39899-8_21

Ming Li, A. Kapoor and R. H. Taylor, "A constrained optimization approach to virtual fixtures," *2005 IEEE/RSJ International Conference on Intelligent Robots and Systems*, Edmonton, AB, Canada, 2005, pp. 1408-1413, doi: 10.1109/IROS.2005.1545420.

Ways to Design H and h

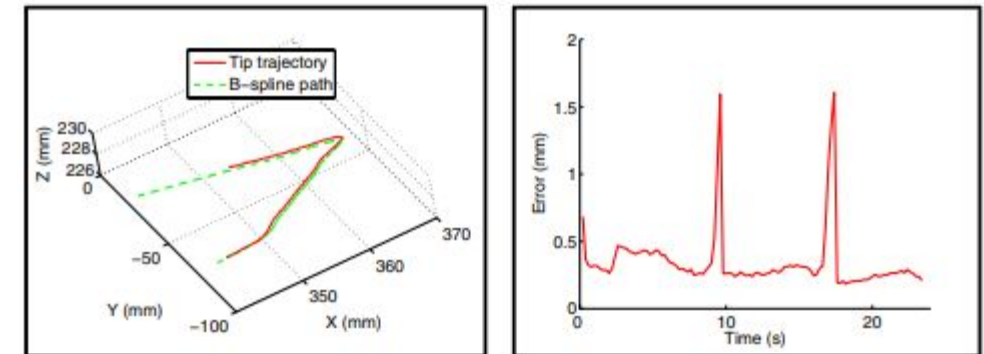
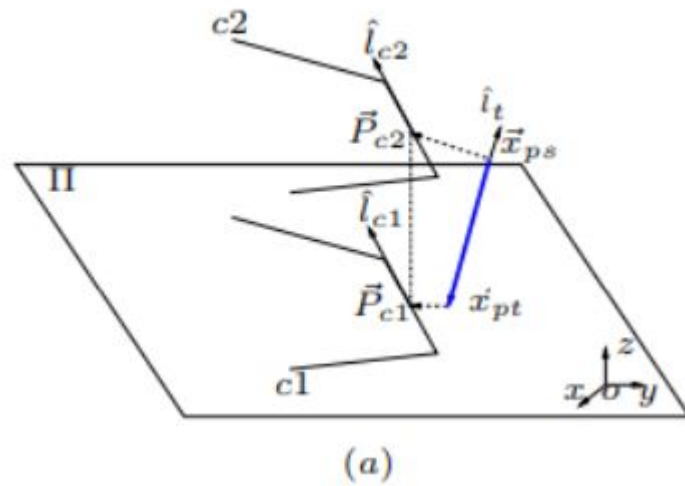
- Stay at a Point
- Maintain a Direction
- Move along a Line
- Rotate around an Axis
- Plan Related Case

$$H = \begin{bmatrix} -c_{\alpha 1} c_{\beta 1}, & -c_{\alpha 1} s_{\beta 1}, & -s_{\alpha 1}, & 0, & 0, & 0 \\ \dots & \dots & \dots & \dots & \dots & \dots \\ -c_{\alpha 1} c_{\beta m}, & -c_{\alpha 1} s_{\beta m}, & -s_{\alpha 1}, & 0, & 0, & 0 \\ \dots & \dots & \dots & \dots & \dots & \dots \\ -c_{\alpha n} c_{\beta 1}, & -c_{\alpha n} s_{\beta 1}, & -s_{\alpha n}, & 0, & 0, & 0 \\ \dots & \dots & \dots & \dots & \dots & \dots \\ -c_{\alpha n} c_{\beta m}, & -c_{\alpha n} s_{\beta m}, & -s_{\alpha n}, & 0, & 0, & 0 \end{bmatrix}, \vec{h} = \begin{bmatrix} -\epsilon_1 \\ \vdots \\ -\epsilon_1 \end{bmatrix} - H\vec{\delta}$$

H and h for Stay at a point

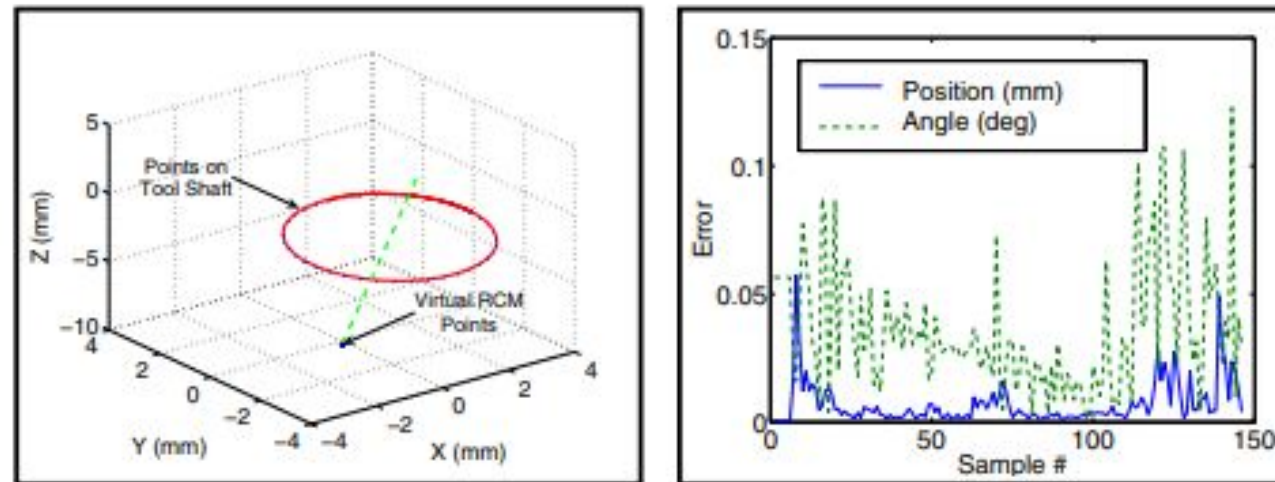
Li, M., Taylor, R.H. (2003). Optimum Robot Control for 3D Virtual Fixture in Constrained ENT Surgery. In: Ellis, R.E., Peters, T.M. (eds) Medical Image Computing and Computer-Assisted Intervention - MICCAI 2003. MICCAI 2003. Lecture Notes in Computer Science, vol 2878. Springer, Berlin, Heidelberg. https://doi.org/10.1007/978-3-540-39899-8_21

Ming Li, A. Kapoor and R. H. Taylor, "A constrained optimization approach to virtual fixtures," *2005 IEEE/RSJ International Conference on Intelligent Robots and Systems*, Edmonton, AB, Canada, 2005, pp. 1408-1413, doi: 10.1109/IROS.2005.1545420.



Li, M., Taylor, R.H. (2003). Optimum Robot Control for 3D Virtual Fixture in Constrained ENT Surgery. In: Ellis, R.E., Peters, T.M. (eds) Medical Image Computing and Computer-Assisted Intervention - MICCAI 2003. MICCAI 2003. Lecture Notes in Computer Science, vol 2878. Springer, Berlin, Heidelberg. https://doi.org/10.1007/978-3-540-39899-8_21

Ming Li, A. Kapoor and R. H. Taylor, "A constrained optimization approach to virtual fixtures," *2005 IEEE/RSJ International Conference on Intelligent Robots and Systems*, Edmonton, AB, Canada, 2005, pp. 1408-1413, doi: 10.1109/IROS.2005.1545420.



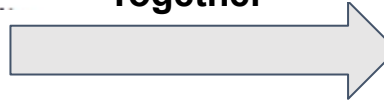
Li, M., Taylor, R.H. (2003). Optimum Robot Control for 3D Virtual Fixture in Constrained ENT Surgery. In: Ellis, R.E., Peters, T.M. (eds) Medical Image Computing and Computer-Assisted Intervention - MICCAI 2003. MICCAI 2003. Lecture Notes in Computer Science, vol 2878. Springer, Berlin, Heidelberg. https://doi.org/10.1007/978-3-540-39899-8_21

Ming Li, A. Kapoor and R. H. Taylor, "A constrained optimization approach to virtual fixtures," *2005 IEEE/RSJ International Conference on Intelligent Robots and Systems*, Edmonton, AB, Canada, 2005, pp. 1408-1413, doi: 10.1109/IROS.2005.1545420.

- Two Components
 - Stay at a Point

$$H_P = \begin{bmatrix} -c_{\alpha 1} c_{\beta 1}, & -c_{\alpha 1} s_{\beta 1}, & -s_{\alpha 1}, & 0, & 0, & 0 \\ \dots & \dots & \dots & \dots & \dots & \dots \\ -c_{\alpha 1} c_{\beta m}, & -c_{\alpha 1} s_{\beta m}, & -s_{\alpha 1}, & 0, & 0, & 0 \\ \dots & \dots & \dots & \dots & \dots & \dots \\ -c_{\alpha n} c_{\beta 1}, & -c_{\alpha n} s_{\beta 1}, & -s_{\alpha n}, & 0, & 0, & 0 \\ \dots & \dots & \dots & \dots & \dots & \dots \\ -c_{\alpha n} c_{\beta m}, & -c_{\alpha n} s_{\beta m}, & -s_{\alpha n}, & 0, & 0, & 0 \end{bmatrix} \quad \vec{h}_p = \begin{bmatrix} -\epsilon_1 \\ \vdots \\ -\epsilon_1 \end{bmatrix} - H\vec{\delta}$$

Together



$$\operatorname{argmin}_{\Delta \vec{q}} \|W \cdot (J(\vec{q}) \cdot \Delta \vec{q} - \Delta x_d)\|$$

or

$$\operatorname{argmin}_{\Delta \vec{q}} \|W \cdot (J(\vec{q}) \cdot \Delta \vec{q} - \Delta x_d - F)\|$$

- Maintain a Direction

$$H_D = \begin{bmatrix} 0, & 0, & 0, & -c_{\alpha 1} c_{\beta 1}, & -c_{\alpha 1} s_{\beta 1}, & -s_{\alpha 1} \\ \dots & \dots & \dots & \dots & \dots & \dots \\ 0, & 0, & 0, & -c_{\alpha 1} c_{\beta m}, & -c_{\alpha 1} s_{\beta m}, & -s_{\alpha 1} \\ \dots & \dots & \dots & \dots & \dots & \dots \\ 0, & 0, & 0, & -c_{\alpha n} c_{\beta 1}, & -c_{\alpha n} s_{\beta 1}, & -s_{\alpha n} \\ \dots & \dots & \dots & \dots & \dots & \dots \\ 0, & 0, & 0, & -c_{\alpha n} c_{\beta m}, & -c_{\alpha n} s_{\beta m}, & -s_{\alpha n} \end{bmatrix} \quad \vec{h}_d = \begin{bmatrix} -\epsilon_1 \\ \vdots \\ -\epsilon_1 \end{bmatrix} - H\vec{\delta}$$

$$\text{s.t.} \quad \begin{bmatrix} H_p \\ H_D \end{bmatrix} \cdot J(\vec{q}) \cdot \Delta \vec{q} \geq \begin{bmatrix} \vec{h}_p \\ \vec{h}_d \end{bmatrix}$$

Li, M., Taylor, R.H. (2003). Optimum Robot Control for 3D Virtual Fixture in Constrained ENT Surgery. In: Ellis, R.E., Peters, T.M. (eds) Medical Image Computing and Computer-Assisted Intervention - MICCAI 2003. MICCAI 2003. Lecture Notes in Computer Science, vol 2878. Springer, Berlin, Heidelberg. https://doi.org/10.1007/978-3-540-39899-8_21

Ming Li, A. Kapoor and R. H. Taylor, "A constrained optimization approach to virtual fixtures," 2005 IEEE/RSJ International Conference on Intelligent Robots and Systems, Edmonton, AB, Canada, 2005, pp. 1408-1413, doi: 10.1109/IROS.2005.1545420.

CONCLUSION

- [1]Gilboy, Kevin Michael. ROBOTIC ULTRASOUND TOMOGRAPHY AND COLLABORATIVE CONTROL. 2020, https://drive.google.com/file/d/19cGn_ZnCLbUESI9dta3l0s91Qdg-DwQl/view?usp=sharing.
- [2]Ting-Yun Fang, Weiqi Wang. Co-Robotic Ultrasound Imaging System. 2017, <https://drive.google.com/file/d/16PvOISm7f2qzwKBoGVO7q6Qlb2Tdrwy/view?usp=sharing>.
- [3]Zerdine, Z.-Skin. Multi-Modality Pelvic Phantom. <https://www.cirsinc.com/wp-content/uploads/2019/04/048A-DS-120418.pdf>.
- [4]Gilboy, Kevin M., et al. Dual-Robotic Ultrasound System for In Vivo Prostate Tomography. 2020, https://link.springer.com/chapter/10.1007/978-3-030-60334-2_16.
- [5]Zhang, Haichong K., et al. 'Phantom with Multiple Active Points for Ultrasound Calibration'. J. Med. Imag. 5(4), 045001 (2018), Doi: 10.1117/1.JMI.5.4.045001., 2022b, <https://pubmed.ncbi.nlm.nih.gov/30525061/>.
- [6]Bray, F., et al. Global Cancer Statistics 2018: GLOBOCAN Estimates of Incidence and Mortality Worldwide for 36 Cancers in 185 Countries. Vol. 68(6), 2018, pp. 394–424.
- [7]Horn, Berthold K. P., et al. 'Closed-Form Solution of Absolute Orientation Using Orthonormal Matrices'. Journal of The Optical Society of America A-Optics Image Science and Vision, vol. 5, 1988, pp. 1127–1135.
- [8]Seifabadi, R. 'Correlation of Ultrasound Tomography to MRI and Pathology for the Detection of Prostate Cancer'. Medical Imaging 2019: Ultrasonic Imaging and Tomography International Society for Optics and Photonics, vol. 10955, 2019, p. 109550C.
- [9]Aalamifar, F. 'Co-Robotic Ultrasound Tomography: A New Paradigm for Quantitative Ultrasound Imaging'. Ph. D. Thesis, Johns Hopkins University, Oct. 2016.

Thank you



JOHNS HOPKINS
UNIVERSITY



JOHNS HOPKINS
SCHOOL of MEDICINE

Phantom with multiple active points for ultrasound calibration

$$\operatorname{argmin}_{X \in SE(3)} \sum_{i=1}^{N-1} \sum_{j=i+1}^N \|B^{(i)} X p^{(i)} - B^{(j)} X p^{(j)}\|_2^2 \quad (\text{or Gradient descent})$$

$$\sigma_{\text{Accu}} = \left\| \frac{1}{N} \sum_{i=1}^N (B_i X p_i - c) \right\|_2, \quad \text{Accuracy}$$

$$\sigma_{RP} = \left\| \sqrt{\frac{1}{N} \sum_{i=1}^N (B_i X p_i - \overline{B X p})^2} \right\|_2, \quad \text{Precision}$$